第 21 卷　第 4 期　　激　光　技　术　　Vol. 21, No. 4
1997 年 8 月　　LASER TECHNOLOGY　　August, 1997

Changes of super-Gaussian beams upon propagation

L　Baida, Wang Xiqing, Zhang Bin
(Institute of Laser Physics and Laser Chemistry, Sichuan University, Chengdu, 610064)

Abstract: Numerical calculations have been performed to describe the propagation of super-Gaussian (SG) beams and the changes in the intensity (amplitude) distribution and phase behavior. The condition has been discussed, under which SG beams preserve their shape and order, while passing through paraxial optical systems.

Key words: super Gaussian beam　propagation and transformation　paraxial optical system

超高斯光束传输中的变化

吕百达　王喜庆　张　彬
(四川大学激光物理与化学研究所, 成都, 610064)

摘要: 为说明超高斯光束的传输特性, 以及光强(振幅)分布的位相的变化, 进行了大量数值计算。还研究了超高斯光束通过近轴光学系统时, 保持其形状和阶数不变的条件。

关键词: 超高斯光束　传输变换　近轴光学系统

ⅳ. Introduction

In recent years great attention has been paid to super-Gaussian (SG) beams due to their importance for some practical applications. So far, the propagation of SG beams and distortions of the on-axis intensity have been studied numerically[1], and analytical expressions by means of a local expansion in Lagurre-Gauss (LG) or Hermite-Gauss (HG) beams has been proposed to characterize the propagation of SG beams[2]. The aim of this paper is to give a detailed study of the changes in both intensity profiles and phase behavior of SG beams upon propagation. The distortions originate from the physical reason that the paraxial wave equation in free space does not admit a SG solution. Fortunately, there exists a condition, under which SG beams retain their shape and order unchanged.

㈦. SG beams are not eigensolutions of the wave equation in free space

It is well-known that the electro-magnetic field $E(r, \theta, z)$ in the stationary state obeys the Helmholtz equation, which, in the cylindrical coordinate system (r, θ, z), is given by

$$\frac{1}{r}\frac{\partial}{\partial r}\left(r\frac{\partial E(r,\theta,z)}{\partial r}\right)+\frac{1}{r^2}\frac{\partial^2 E(r,\theta,z)}{\partial\theta^2}+\frac{\partial^2 E(r,\theta,z)}{\partial z^2}+k^2E(r,\theta,z)=0 \qquad (1)$$

where k denotes the wave number, $k=2\pi/\lambda$ (λ—wavelength). If E is independent of θ, Eq. (1) is simplified to

$$\frac{1}{r}\frac{\partial}{\partial r}\left(r\frac{\partial E(r,\theta,z)}{\partial r}\right)+\frac{\partial^2 E(r,\theta,z)}{\partial z^2}+k^2E(r,\theta,z)=0 \qquad (2)$$

Consider an initial field in the place of $z=0$ which takes the form of SG beams

$$E(r, z=0)=\exp[-(r/w_0)^n] \tag{3}$$

where w_0 and n $(n>2)$ are the waist radius and order of SG beams, and in two limiting cases of $n=2$ and ∞, Eq. (3) describes the Gaussian beam and plane wave, respectively. Thus, for an arbitrary propagation distance, say z, the field $E(r, z)$ is assumed to become

$$E(r, z)=f_1(z)\exp[-f_2(z)(r/w_0)^n] \tag{4}$$

with

$$f_1(0)=f_2(0)=1 \tag{5}$$

The substitution from Eq. (4) into Eq. (2) and comparison of the terms r/w_0 with the same order $(n>2)$ yield

$$f_1(z)f_2(z)=0 \quad \text{for } (r/w_0)^{n-2} \tag{6a}$$

$$2\frac{df_1(z)}{dz}\frac{df_2(z)}{dz}+f_1(z)\frac{df_2^2(z)}{dz^2}=0 \quad \text{for}(r/w_0)^n \tag{6b}$$

$$f_1(z)f_2^2(z)=0 \quad \text{for}(r/w_0)^{2(n-1)} \tag{6c}$$

$$f_1(z)[df_2(z)/dz]^2=0 \quad \text{for}(r/w_0)^{2n} \tag{6d}$$

It can be readily seen from Eq. (6) that the solution of the form Eq. (4) is not admissible for the wave equation (2) because Eq. (6a) and Eq. (6c) directly contradict Eq. (5).

Furthermore, in the paraxial approximation Eq. (2) becomes

$$\frac{\partial^2 E'(r, z)}{\partial r^2}+\frac{1}{r}\frac{\partial E'(r, z)}{\partial r}-2ik\frac{\partial E'(r, z)}{\partial z}=0 \tag{7}$$

with $E(r, z)=E'(r, z)\exp(-ikz)$. The similar way as above leads to

$$f_1(z)f_2(z)=0 \tag{8}$$

Thus, we have shown that SG beams are not solutions of the Helmholtz equation and the paraxial wave equation, but apparently, two limiting forms of $n=2$ and $n=\infty$ are the solutions Eq. (7) and Eq. (2), respectively.

四、Propagation of SG beams

The propagation of SG beams in free space is characterized by the Huygens-Fresnel diffraction integral

$$E_2(r_2, z)=\frac{ik}{z}\exp[ik(z+\frac{r_2^2}{2z})]\int_0^{+\infty}E(r_1, 0)J_0(\frac{kr_1r_2}{z})\exp(\frac{ikr_1^2}{2z})r_1dr_1 \tag{9}$$

with J_0 being the Bessel function of the zero order. On substituting from Eq. (3) into Eq. (9) and after some algebras, we obtain the field distribution $E_2(r_2, z)$ of SG beams passing through a distance z in free space

$$E_2(r_2, z)=F(r_2, z)\exp[i(kz+\phi(r_2, z))] \tag{10}$$

where

$$F(r_2, z)=2\pi N_w\int_0^{+\infty}v\exp(-v^n)J_0(2\pi N_w v\frac{r_2}{w_0})\exp(i\pi N_w v^2)dv \tag{11}$$

$$\phi(r_2, z)=\frac{kr_2^2}{2z}+\arg\left\{\int_0^{+\infty}v\exp(-v^n)J_0(2\pi N_w v\frac{r_2}{w_0})\exp(i\pi N_w v^2)dv\right\} \tag{12}$$

and N_w is the Fresnel number associated with the beam

$$N_w=w_0^2/\lambda z \tag{13}$$

From Eq. (11) the intensity distribution $I(r_2, z)$ is readily obtained, which is given by

$$I_2(r_2, z)=F(r_2, z)F^*(r_2, z) \tag{14}$$

Numerical calculations were performed on a 486 computer, using Simpson's method and Eq.

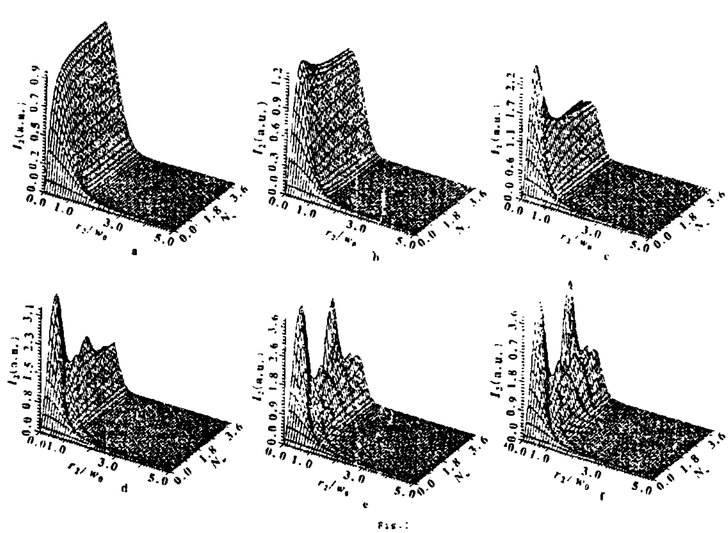

Fig. 1 The intensity distribution $I_2(r_2, z)$ (arbitrary units) as a function of the normalized radial coordinate r_2/w_0 and the Fresnel number N_w

a—$n=2$ b—$n=3$ c—$n=6$ d—$n=12$ e—$n=36$ f—$n=100$

(11), (12) and (14). Typical results are compiled in Figs. 1, 2 and 3, the results for the Gaussian beam is depicted together for the convenience of comparison. Fig. 1 gives the intensity distribution $I_2(r_2, z)$ of SG beams as a function of the normalized radial coordinate r_2/w_0 and the Fresnel number N_w, showing the distortions in both radial and axial intensity profiles. Assume that $w_0=1$mm and $\lambda=1\mu$m, from Fig. 2, where the radial intensity profiles of SG beams are represented for different propagation distances z (i.e., N_w) and SG orders n, we see clearly that for the near propagation distances, for example, $z=1$m, 0.5m, 0.1m, corresponding to $N_w=1, 2, 10$, the distortions increase with increasing n, the dips and ripples in intensity profiles are observable for higher-order SG beams. Nevertheless, the Gaussian beam retains its form unchanged upon propagation ($n=2$ in Fig. 1a, 2). On the other hand, for the far propagation distances, e.g., $z=10$m ($N_w=0.1$) intensity profiles of SG beams with different orders n become more smooth, and approach the Frauhofer diffraction pattern. Similar behavior is seen in the phase profiles of SG beams shown in Fig. 3, where the phase $\psi(r_2, z)$ is plotted against r_2/w_0 for different n and N_w.

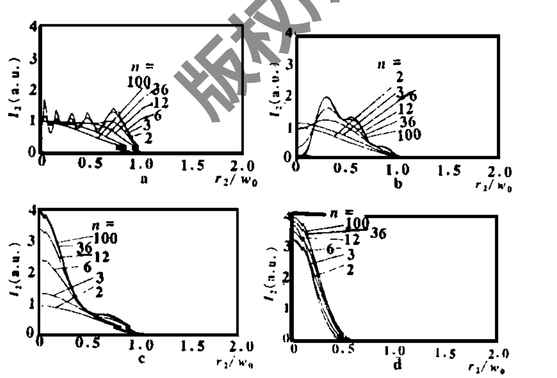

Fig. 2 The radial intensity profiles $I_2(r_2, z)$ (a.u.) are represented for $n=2, 3, 6, 12, 36$ and 100

a—$N_w=10$ b—$N_w=2$ c—$N_w=1$

d—$N_w=0.1$

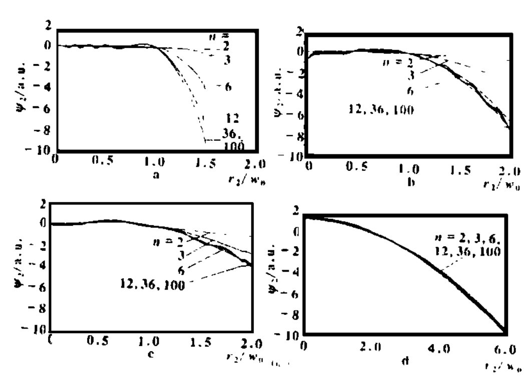

Fig. 3 The phase $\psi(r_2, z)$ is plotted against r_2/w_0 for $n=2, 3, 6, 12, 36$ and 100

a—$N_w=10$ b—$N_w=2$ c—$N_w=1$

d—$N_w=0.1$

㊄ The condition that SG beams preserve their shape and order upon propagation

The above analysis has shown that SG beams undergo distortions while propagating even in free space, which is not desirable for the practical purpose. Obviously, a question arises: Can SG beams preserve their shape and order on a certain condition? It is well-known that the beam propagation through a paraxial optical system with a transfer matrix $\begin{bmatrix} A & B \\ C & D \end{bmatrix}$ is characterized by the generalized Huygens-Fresnel diffraction integral

$$E_2(x_2, y_2, z) = [i/(\lambda B)]\exp(ikz)\iint E_1(x_1, y_1, z=0)\exp\{[ik/(2B)][A(x_1^2+y_1^2) - 2(x_1x_2+y_1y_2) + D(x_2^2+y_2^2)]\}\mathrm{d}x_1\mathrm{d}y_1 \qquad (15)$$

Letting $B=0$ in Eq. (15) and recalling the formula of the δ-function

$$\delta(x, y) = \lim_{P\to\infty}(P^2/\pi)\exp[-P^2(x^2+y^2)] \qquad (16)$$

and the relation of $ABCD$ matrix elements

$$AD - BC = 1 \qquad (17)$$

lead to

$$E_2(x_2, y_2, z) = (1/A)\exp\{ik[z + (C/2A)(x_2^2+y_2^2)]\}E_1(x_2/A, y_2/A) \qquad (18)$$

On substituting from Eq. (3) into Eq. (18), in the cylindrical coordinate system we obtain

$$E_2(r_2, z) = (1/A)\exp\{ik[z + (C/2A)r_2^2]\}\exp\{-[r_2/(|A|w_0)]^n\} \qquad (19)$$

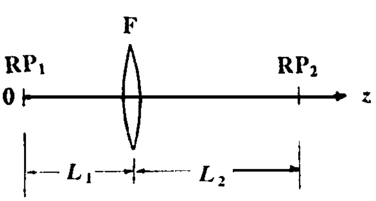

Fig. 4　A lens imaging system

Thus, after passing though optical imaging systems of $B=0$, SG beams retain their shape and order unchanged, but amplified (or squeezed) by a factor $1/A$, the spot radius becomes $w_0|A|$ and the phase is radially modulated by a term $(C/2A)r_2^2$.

A simple example of the imaging system is shown in Fig. 4, where L_1 and L_2 are the distances between the object plane RP_1 and thin lens F, the image plane RP_2 and F, respectively. The transfer matrix M from RP_1 to RP_2 reads

$$M = \begin{bmatrix} A & B \\ C & D \end{bmatrix} = \begin{bmatrix} 1 - L_2/f & L_1 + L_2 - L_1L_2/f \\ -1/f & 1 - L_1/f \end{bmatrix} \qquad (20)$$

with f being the focal length of the lens. By letting $B=0$ we have

$$1/L_1 + 1/L_2 = 1/f \qquad (21)$$

which is the well-known imaging equation of the lens. The SG beams of the form Eq. (3), after propagating through the lens imaging system from $RP_1(z=0)$ to $RP_2(z=L_1+L_2)$, become

$$E_2(r_2, L_1+L_2) = (-L_1/L_2)\exp\{ik[(L_1+L_2) + (L_1/2L_2f)r_2^2]\}\exp\{-[(L_1r_2)/(w_0L_2)]^n\} \qquad (22)$$

(九). Conclusion

In conclusion we have studied the propagation characteristics of SG beams. Although it is possible to give approximate expressions of SG beams by means of LG or HG beams[2], the essential distinction between them should be noted, i.e., SG beams are not eigensolutions of the

激光相变硬化工艺参数的选择

任恩扬　陈铁力　林　渝　李俊昌
(昆明理工大学激光应用研究所, 昆明, 650093)

摘要: 激光在工业应用中, 相变硬化是一个重要方面。其工艺选择直接影响着相变硬化层的深度和宽度。

从热传导基本方程出发, 得出了相变硬化过程中工艺参数(激光功率、光斑直径、离焦量、扫描速度) 与硬化层深度、宽度之间的关系。用编制的工艺参数选择的计算机软件计算的结果与实验结果进行了比较, 其相对误差为: 硬化层宽度平均相对误差为 3.7%, 硬化层深度为 18.7%。

关键词: 激光　相变硬化　工艺参数

Selecting technological parameters from laser induced phase transformation hardening processes of materials

Ren Enyang, Chen Tieli, Lin Yu, Li Junchang
(Institute of Laser Application, Kunming Institute of Technology, Kuming, 650093)

Abstract: We solve the heat conduction equation with semi-infinite boundary condition and present a mathematical model to emulate the relationship of the technical parameters ω (beam radius), v (scanning speed) and P (laser power) of phase transformation processing to depth and width of the hardened region. The comparisons of emulation with tested results show that the average relative errors of width and depth of hardened region are 3.7% and 18.7%, respectively. This results are meaningful for better selection of technical parameter.

Key words: laser　phase transformation hardening　technological parameter

paraxial wave equation in free space. Fortunately, SG beams preserve their shape and order, while propagating through optical imaging systems, which would be useful for some practical applications. Finally, we would like to point out that the results in sections 3 and 4 are valid for the unapertured case. The propagation properties of apertured SG beams will be published elsewhere.

This work was supported by the National Hi-Tech Foundation of China.

References

1　Partent A, Morin M, Lavigne P. Opt & Quant Electron, 1992; 24: 1071～1079
2　Palma C, Bagini V. Opt Commun, 1994; 111: 6～10

*　　*　　*

作者简介: 吕百达, 男, 1943 年出生。教授, 博士生导师。主要研究方向为新型和高功率固体激光器件与技术, 光腔物理与光束传输变换。

收稿日期: 1995-12-03　　收到修改稿日期: 1996-04-20